

Analysis of Finite Conductivity Cylindrical Conductors Excited by Axially-Independent TM Electromagnetic Field

ANTONIJE R. DJORDJEVIĆ, TAPAN K. SARKAR, SENIOR MEMBER, IEEE,
AND SADASIVA M. RAO, MEMBER, IEEE

Abstract — A method is presented for the analysis of a system of cylindrical conductors, of large but finite conductivity, situated in a uniform dielectric and excited by an axially-independent TM electromagnetic field. The analysis is based on separating the space into the region exterior to the conductors and regions interior to the conductors, placing equivalent electric and magnetic currents on the boundary surfaces, applying the boundary conditions for the tangential fields and, hence, obtaining a system of coupled integral equations. Due to the special geometry and the chosen excitation, the problem treated is a two-dimensional one. The distribution of the unknown surface currents is approximated by pulses, and the amplitudes of these pulses are determined by a point-matching technique. This method is applied to the problem of determining the inductance and resistance of two-wire transmission lines.

I. INTRODUCTION

THE USUAL WAY OF determining the inductance and resistance of transmission lines, which are needed for the quasi-TEM analysis, is by using the following technique. As the first step, the line conductors are assumed to be made of a perfectly conducting material, and the inductance matrix is computed by inverting the capacitance matrix (obtained for the case when the dielectric of the line is a vacuum) [1]–[2]. Such an approach is only approximate, because it does not consider the magnetic energy stored within conductors, which can be very important at lower frequencies (towards the dc end of the spectrum). In addition, it assumes that the proximity and end effects are fully developed, which is, in reality, the case only at higher frequencies, when the skin effect is pronounced, thus yielding the current distribution which is not accurate at lower frequencies. As the consequence of such a procedure, the resulting inductance matrix is frequency independent.

Regarding the resistance, in the conventional approach it is obtained by perturbing the perfect-conductor case, i.e., by using the surface resistance of the conductor, assuming

Manuscript received February 3, 1985; revised May 22, 1985. This work was supported in part by the Digital Equipment Corporation, Marlboro, MA 01752.

A. R. Djordjević is with the Department of Electrical Engineering, University of Belgrade, P.O. Box 816, 11001 Belgrade, Yugoslavia.

T. K. Sarkar is with the Department of Electrical and Computer Engineering, Syracuse University, Syracuse, NY 13210.

S. M. Rao is with the Department of Electrical Engineering, Rochester Institute of Technology, P.O. Box 9887, Rochester, NY 14623.

that the skin effect is well developed. The resistance thus obtained is, therefore, inadequate to represent the low-frequency behavior of the line. In the low-frequency region, the resistance is almost frequency independent and equal to the dc resistance, while the resistance obtained by the perturbation technique tends to zero as the square root of the frequency.

The problem treated in this paper is a special case of a more general class of problems of numerically finding the electromagnetic field in a system which consists of a number of homogeneous regions, separated by arbitrary boundary surfaces. In other words, the medium is piecewise homogeneous. Generally, the equations describing such a system can be formulated in two ways [3]. Following the first approach, one has to take the volume conduction currents, the volume magnetization and polarization currents, and the surface magnetization currents and polarization charges as the sources of the electromagnetic field.

According to the second approach, by using the electromagnetic-field theorems [3], [4] one can separate the space into a number of homogeneous regions and treat one region at a time, excluding the rest of the system by placing equivalent electric and magnetic currents at the surfaces bounding the regions. If the problem is solved starting from the integral equations for the unknown source distribution, the surface-current formulation is superior over the volume formulation in having a much smaller number of unknowns and yielding surface, rather than volume, integrals that have to be numerically evaluated. Altogether, this results in a much more efficient computer program, regarding both memory requirements and CPU running time.

The equivalent surface-current approach is adopted here for the analysis of the system sketched in Fig. 1. The system under consideration consists of a number of cylindrical conductors of arbitrary cross section. Their conductivity is assumed to be large, but finite, so that the polarization current can be neglected, i.e., so that the material can be described by the complex permittivity $\epsilon = -j\sigma/\omega$. The material is assumed to be nonferromagnetic and homogeneous within each of the cylinders. The cylinders are situated in a homogeneous, lossless dielectric, of parameters ϵ and μ_0 , and excited by an impressed field, which is

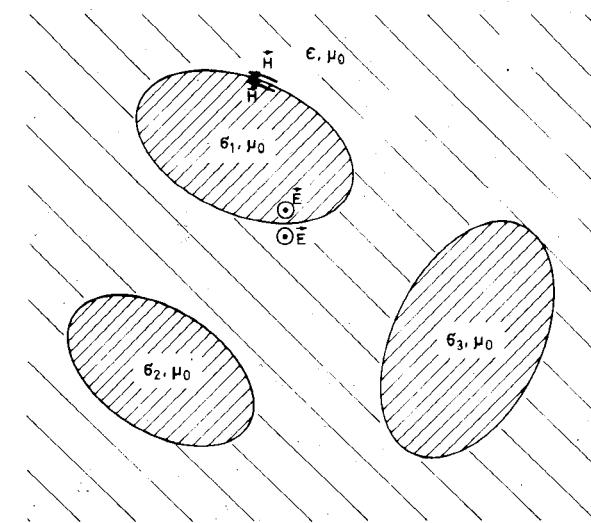
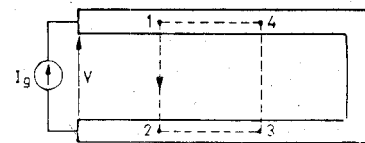


Fig. 1. Sketch of the analyzed system cross section.

uniform along any line parallel to the z -axis. In addition, it is assumed that the impressed electric field is parallel to the z -axis, while the magnetic field is transversal to it, i.e., the excitation is of the TM type.

Such an impressed field requires certain additional clarifications, i.e., we have to know what is its relation to a two-wire transmission-line case. Let us, therefore, consider an electrically short transmission line (i.e., shorter than about 0.01 wavelength), short-circuited at one end, and driven by a sinusoidal ideal current generator at the other end (see Fig. 2). The line represents an impedance as seen from the generator, and, therefore, there is a voltage between the generator terminals, as indicated in Fig. 2. Of course, this voltage is much smaller than would be in the case when the line is matched rather than short-circuited, because the line is electrically short. To the first approximation, the current along the conductors is constant. (More precisely, it is proportional to $\cos kx$, where k is the phase coefficient, and x is the distance from the short circuit towards the generator, if the line losses are relatively small.) However, the voltage between the conductors decreases practically linearly along the line, and drops to zero at the short circuit. (Again, more exactly, the voltage is proportional to $\sin kx$.) The voltage between the conductors (which is defined for a line cross section) is, essentially, the integral of the electric field due to the charges induced on the line conductors, because only these charges give a transversal electric-field component. This field is equal to $-\nabla V$, where V is the electric scalar-potential due to the charges. On the other hand, the line integral of $-\nabla V$ along the path shown in Fig. 2 is zero. Since the integrals along the lines 1-2 and 3-4 do not cancel each other (the voltage being smaller going towards the short circuit), it follows that there must exist a component of $-\nabla V$ along each of the conductors, and that these components are in the direction of the current flow, i.e., opposite in the two conductors. Of course, since the voltage is linearly decreasing going towards the short circuit, these compo-

Fig. 2. Sketch of an electrically short, short-circuited, two-wire transmission line, driven by a generator, with the path 1-2-3-4-1 along which the line integral of $-\nabla V$ is considered.

nents should be uniform along the line. Also, since there is no transversal electric-field component in the conductors (because the current has only the axial component, and the electric-field vector is, in a conductor, always colinear with the current-density vector), the $-\nabla V$ term is axial and uniform over the cross section of each of the conductors.

In our model, we are going to assume that the current is exactly uniform along the transmission-line length. Therefore, no charge can be associated with it, according to the continuity equation. On the other hand, we have to take into account the field due to the charges, as discussed above. To circumvent this difficulty, we take the field due to the charges as the impressed field (i.e., the field that represents the excitation to our system). This field has, of course, to be axial and uniform within each of the conductors. It is worth noting that such a uniform field can be considered as produced by a uniform solenoidal sheet of magnetic currents, wrapping each of the conductors. These currents have only the transversal component, and the electric field produced by them is dual to the magnetic field produced by a similar sheet of electric currents. In the quasi-static case considered here (i.e., the transversal dimension of the transmission line being much smaller than the wavelength in a vacuum), the electric field in the interior of a magnetic-current solenoid is practically uniform and axial, and it is negligible in the exterior of the solenoid. The impressed field in our model is, finally, computed as due to such solenoidal magnetic-current sheets, which are, however, not sketched in Fig. 1.

II. FUNDAMENTAL EQUATIONS

Under the assumptions described in the previous section, no quantity describing the electromagnetic field depends on the z -coordinate, i.e., we have a two-dimensional case. In addition, the currents induced in the conductors have only the z -component (and, of course, their density depends only on the transversal coordinates). Hence, the divergence of these currents is zero, and there are no volume charges in the conductors, nor are there surface charges at the interfaces between the conductors and the dielectric. It is not hard to see that the electric field produced by these currents has only the z -component and the magnetic field has only the transversal component at any point of the system.

We are going to consider the impressed field as the field due to any known sources. In the system considered, the sources of the impressed field are in the dielectric. For example, if we assume the impressed field to be a plane

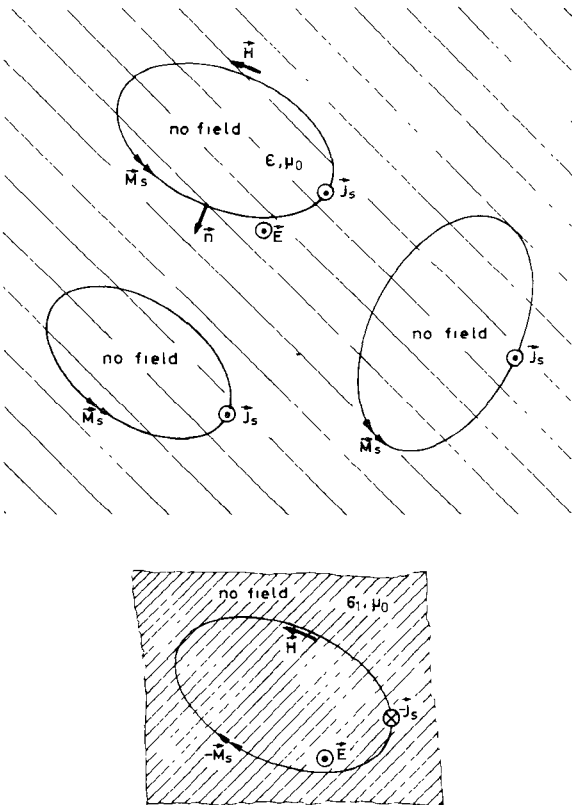


Fig. 3. Systems equivalent to the one in Fig. 1: (a) outside the conductors and (b) inside conductor #1.

electromagnetic wave, the sources are, theoretically, at infinity.

Let us, first, consider the electromagnetic field in the dielectric. Using the equivalence theorem, we can exclude the electromagnetic field in the conductors by introducing equivalent surface electric and magnetic currents at the conductor boundaries, as shown in Fig. 3(a). In this equivalent system, the field in the dielectric remains unchanged, as compared to the field in the original system, while the field in the conductors is zero. The densities of the equivalent currents are related to the (total) tangential electric and magnetic fields at the surface of the conductors (i.e., observed in the dielectric), as

$$\mathbf{J}_s = \mathbf{n} \times \mathbf{H} \quad (1)$$

$$\mathbf{M}_s = \mathbf{E} \times \mathbf{n} \quad (2)$$

where \mathbf{n} is the outward normal to the conductor surfaces. The electromagnetic field in the conductors being zero, we can now substitute the medium of the conductors by the surrounding dielectric, thus homogenizing the medium everywhere. In such a system, the only sources of the electromagnetic field are the equivalent surface electric and magnetic currents, in addition to the sources of the impressed field. Thus, we have at any point for the total electric and magnetic fields

$$\mathbf{E} = -j\omega\mathbf{A} - \frac{1}{\epsilon} \operatorname{curl} \mathbf{F} + \mathbf{E}_i \quad (3)$$

$$\mathbf{H} = -j\omega\mathbf{F} - \operatorname{grad} V_m + \frac{1}{\mu_0} \operatorname{curl} \mathbf{A} + \mathbf{H}_i \quad (4)$$

where ω is the angular frequency, \mathbf{E}_i and \mathbf{H}_i describe the impressed field

$$A = \mu_0 \int_s \mathbf{J}_s g(r) ds \quad (5)$$

is the magnetic vector-potential

$$F = \epsilon \int_s \mathbf{M}_s g(r) ds \quad (6)$$

is the electric vector-potential, and

$$V_m = \frac{1}{\mu_0} \int_s \rho_{ms} g(r) ds \quad (7)$$

is the magnetic scalar-potential. In (5)–(7) $g(r)$ is Green's function for the two-dimensional case (i.e., corresponding to an infinitely long, straight, uniform line source), s is the contour of the conductor cross sections, r is the distance between the field and source points (both lying in the same transversal plane) and ρ_{ms} is the surface magnetic-charge density. Green's function for this case is [3]

$$g(r) = -\frac{j}{4} H_0^{(2)}(kr) \quad (8)$$

where $H_0^{(2)}$ is Hankel's function of the second kind and order zero, and $k = \omega/\epsilon\mu_0$ is the phase coefficient. It is worth noting that, in the limiting quasi-static case, Green's function tends to $-(1/2\pi)\log(kr)$.

We can now consider the electromagnetic field in the interior of one conductor at a time. We can thereby exclude the field in the dielectric and the other conductors by wrapping the conductor by equivalent surface electric and magnetic currents. These currents are exactly opposite to those given by (1) and (2), as presented in Fig. 3(b). According to the equivalence theorem, the field exterior to the conductor is now zero, so that this exterior region can be assumed to be filled with the material the conductor is made of. In other words, we have now homogenized the entire space, which enables us to use the usual expressions for the fields and retarded potentials, (3)–(7). However, in this case, the permittivity should be substituted by the complex permittivity, $\hat{\epsilon} = -j\sigma/\omega$, while Green's function is now

$$g(r) = \frac{1}{2\pi} (\operatorname{ker}(|\gamma|r) + j \operatorname{kei}(|\gamma|r)) \quad (9)$$

where ker and kei are Kelvin's functions and $\gamma = \sqrt{j/\sqrt{\epsilon\mu_0\sigma}}$ is the propagation coefficient in the conductor. Also, in this case $\mathbf{E}_i = 0$ and $\mathbf{H}_i = 0$.

The unknown distributions of electric and magnetic currents have to be determined so that the electromagnetic field be zero in the space in Fig. 3(a) which corresponds to the conductors in Fig. 1, and also that it be zero in the space in Fig. 3(b) which corresponds to the dielectric in Fig. 1. According to the uniqueness theorem, we can postulate that either the electric field or the magnetic field tangential to the boundary of the zero-field region be zero (at the side of the boundary interior to the region). Although, theoretically, these two conditions are equivalent, our choice was based on the considerations that the method can cover as broad a frequency range as possible. To that purpose, the

frequency behavior of the terms in (3) and (4) should be inspected for both systems of Fig. 3(a) and (b). Thereby, the low-frequency end is more critical, because at higher frequencies the terms in (3) and (4) are better balanced.

At lower frequencies, the term $-j\omega A$, due to a current filament, is practically proportional to the frequency f to the first power for both systems, and the terms $1/\epsilon \operatorname{curl} F$ and $1/\mu_0 \operatorname{curl} A$ are almost frequency-independent. The term $-j\omega F$ is proportional to f^1 in the system of Fig. 3(a), while it is frequency-independent in the system of Fig. 3(b). (Note that the electric-current filament in these considerations carries an axial current, while the magnetic-current filament carries a transversal current. In the latter case, magnetic charges must be associated with the magnetic current in order to satisfy the continuity equation.) Finally, the term $\operatorname{grad} V_m$ is frequency-independent for a given line magnetic charge. However, this charge is proportional with a factor $1/f$ to a given magnetic current.

The impressed electric field at a conductor surface is practically uniform and frequency-independent (for a given magnetic-current sheet). However, the impressed magnetic field, due to the same source, is proportional to f^1 . In addition, at low frequencies, the current density and, hence, the electric field within a conductor is uniform. As a consequence, the equivalent magnetic currents at the conductor surface are of constant intensity and in phase with the equivalent electric currents. By inspecting (4) and noting that $\rho_{ms} = j/\omega \operatorname{div}_s \mathbf{M}_s$, it can be seen that this equation might be numerically unstable because of the great difference in magnitudes of the four terms in the system of Fig. 3(a). Therefore, the boundary condition for the tangential electric field was adopted for the external problem. At the same time, the system of Fig. 3(b), the $\operatorname{curl} F$ term produces no field external to the magnetic-current sheet, but this result is obtained as the sum of large, opposite terms, which greatly exceed in magnitude the $-j\omega A$ term. Thus, at very low frequencies, (3) might be numerically unstable. However, in (4), a similar problem arises because the $\operatorname{grad} V_m$ can be very large, unless the magnetic currents are forced to have a uniform intensity around the conductor boundary. Nevertheless, the boundary condition for the tangential magnetic field was used for the internal problem, because it was considered to give a more natural behavior of the equivalent currents than (3).

III. APPROXIMATE SOLUTION

In order to numerically obtain the solution to the coupled equations (3) and (4), the first of them formulated for the exterior, and the second for the interior problem, the point-matching method was applied [5] with a piecewise constant (i.e., pulse) approximation of the unknown distributions of electric and magnetic currents. To that purpose, each of the interfaces was divided into a number of strips, running parallel to the z -axis, and the electric and magnetic currents were assumed to be uniform over each of the strips. Note that such an approximation yields magnetic charges only along the edges of the strips, because $\operatorname{div}_s \mathbf{M}_s = 0$ over a strip. The matching points were allocated at

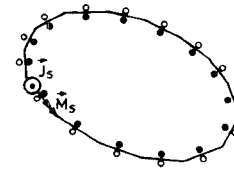


Fig. 4. Segmentation of the boundary surfaces of the system of Fig. 1: electric and magnetic-current pulses and matching points \dots for the exterior and $\circ \circ \circ$ for the interior problem.

middle points of the segments representing strip cross sections at a transverse plane, as sketched in Fig. 4.

The curls in (3) and (4) were evaluated by introducing the “curl” operator under the integrals, where they operate on the kernels only, yielding

$$\operatorname{grad} g(r) = \frac{dg}{dr} \mathbf{i}_r \quad (10)$$

where \mathbf{i}_r is the unit vector of the vector \mathbf{r} .

After some simple manipulations and using the properties of Hankel's and Kelvin's functions, the integrals which have to be evaluated in our case are reduced to the forms

$$-j\omega A = -j\xi \mathbf{J}_s \int_s -\frac{j}{4} H_0^{(2)}(kr) d(ks) \quad (11)$$

$$\frac{1}{\epsilon} \operatorname{curl} F = -\mathbf{M}_s \times \int_s \frac{j}{4} H_1^{(2)}(kr) \mathbf{i}_r d(ks) \quad (12)$$

for the exterior problem, and

$$-j\omega F = -j \frac{\mathbf{M}_s}{|\xi|} \int_s \frac{1}{2\pi} (\operatorname{ker}(|\gamma|r) + j \operatorname{kei}(|\gamma|r)) d(|\gamma|r) \quad (13)$$

$$\frac{1}{\mu_0} \operatorname{curl} A = -\sqrt{j} \mathbf{J}_s \int_s \frac{1}{2\pi} (\operatorname{ker}'(|\gamma|r) + j \operatorname{kei}'(|\gamma|r)) \mathbf{i}_r d(|\gamma|r) \quad (14)$$

for the interior problem. In (11)–(14), \mathbf{J}_s and \mathbf{M}_s are current densities of a strip, s is its cross section, and $\xi = \sqrt{\mu_0/\epsilon}$ and $\hat{\xi} = \sqrt{j/\sqrt{\omega\mu_0\sigma}}$ are the intrinsic impedances of the dielectric and conductor, respectively. Regarding the magnetic scalar-potential, its gradient is merely reduced to the form

$$\operatorname{grad} V_m = - \left[\frac{j}{2\pi|\xi|} (\operatorname{ker}(|\gamma|r) + j \operatorname{kei}(|\gamma|r)) \mathbf{i}_r \right]_{r=r_1}^{r_2} \quad (15)$$

where r_1 and r_2 are the distances between the field point and the ends of the strip cross section.

At higher frequencies, when the widths of the strips become much greater than the skin-depth $\sqrt{2/\omega\mu_0\sigma}$, the magnetic field at a matching point in the interior problem is practically due only to the electric and magnetic currents in the immediate vicinity of that point, i.e., only to the local surface currents. In that case (4), (13), and (14) should yield

$$M_s/J_s = \hat{\xi} \quad (16)$$

for any strip, which could be expected from the analysis of

field penetration into a conductor at high frequencies. This result has been verified numerically, thus checking the integration procedure.

In order to numerically evaluate the terms in (11)–(14), one has to be careful about the case when the field point is on the strip, the field of which is computed, since, in that case, the kernel in (5) and (6) has an integrable singularity. Even more critical is the singularity in the curls of the potentials. This problem was alleviated by subtracting from the kernel the dominant term $-1/2\pi \log(r)$, which is the same for both the exterior and interior problems. The integrals associated with this extracted term can be evaluated explicitly, as shown in the Appendix, while the remainder was evaluated numerically, using the Gauss–Legendre integration scheme of the eighth order. Thereby, the cross section of a strip should be divided into subsegments the length of which is, at most, equal to one wavelength for the exterior problem, namely a few skin depths for the interior problem, and the integration formula should be applied to each of these subsegments.

IV. NUMERICAL EXAMPLES

The procedure described in Sections II and III was applied to a special case of two identical, parallel rectangular conductors, placed as sketched in Fig. 5. Each of the conductors was assumed to be in a uniform axial impressed field. The intensities of the impressed field for each of the conductors are equal, but the directions of the fields are opposite. Such a case practically exists with an electrically short transmission line of finite conductivity driven at one end by a generator and short circuited at the other end. The sources of the impressed field in this case are charges, located at the conductor surfaces (as well as the generator terminals). The charge density per unit length is practically linearly diminishing from the generator toward the short circuit. If the transverse dimensions of the line are much smaller than the line length, the field due to the charges at the line ends can be neglected around the middle of the line. Also neglecting the retardation, the z -component of the electric field at a level z due to the charges is given by the relation

$$\begin{aligned} E_z &= -\frac{1}{4\pi\epsilon_0} \int_{z_1}^{z_2} \int_{s_t} \rho_s(s, z') \frac{\partial}{\partial z} \left(\frac{1}{r} \right) ds dz' \\ &= \frac{1}{4\pi\epsilon_0} \int_{z_1}^{z_2} \int_{s_t} \frac{\partial \rho_s}{\partial z'} \frac{1}{r} ds dz' \\ &\quad - \left[\frac{1}{4\pi\epsilon_0} \int_{s_t} \rho_s(s, z') \frac{1}{r} ds \right]_{z'=z_1}^{z_2} \end{aligned} \quad (17)$$

since $\partial r/\partial z = -\partial r/\partial z'$. In (17), z_1 and z_2 are the charge boundaries along the z -axis ($z_1 < z < z_2$), s_t denotes the contours of the conductor cross sections, and r is the distance between the field and the source points. Obviously, the last term in (17) can be neglected if the ends (z_1 and z_2) are far away from the field point. Hence, it can be concluded that the z -component of the field due to the charges, which can be considered as the impressed field in

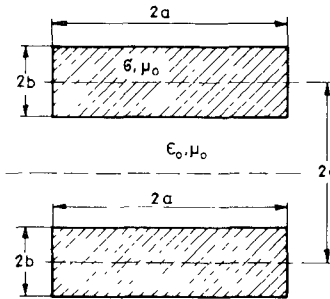


Fig. 5. Cross section of a two-conductor transmission line.

our case, is of the same form as the potential due to these charges. (Note that we are assuming the current distribution to be uniform along the conductor length, and thus no charges can be associated with it, which is, of course, only an approximation.) Only, instead of the charges in the expression for the potential, we have to put the charge derivatives with respect to the z -coordinate. As a result, the impressed field is uniform over the cross section of one conductor, and the directions of the impressed field are opposite in the two conductors.

In the computer program prepared for the present analysis, the impressed field was not taken to be exactly uniform, but rather it was taken to be due to two uniform layers of transverse magnetic currents wrapping the two conductors.

The impedance per unit length is defined as the ratio of the incident electric field divided by the total current across the cross section of the conductor. The total current is obtained by integrating the surface-current density along the cross-section circumference.

As the first example, the dimensions of the system shown in Fig. 5 were adopted to be $a = 1$ mm, $b = 0.1$ mm, and $c = 0.5$ mm. In this, as well as in the other case, the conductor conductivity was 56 MS/m. In Fig. 6, the resistance and inductance per unit length are shown versus frequency, where $R'(0)$ denotes the low frequency resistance value. It can be seen that the resistance starts changing from the dc value when the longer side of the conductor cross section becomes a substantial fraction of the skin depth. However, only when the shorter side becomes close to the skin depth, the resistance exhibits the well-known square-root behavior. At very high frequencies, the resistance starts rapidly increasing. In our model, this is to be attributed to the radiation resistance of the system. It is worth noting that the system shown in Fig. 5 radiates because the current distribution is uniform along the z -axis unlike an ideal TEM transmission line, where the current distribution is sinusoidal, and thus no radiation occurs. The inductance does not change very much with frequency, because of two reasons. First, the thickness of the conductors is very small, so that the internal inductance is negligible. Second, at very low frequencies, the current is uniformly distributed along the wider side of the conductor, as in the dc case, but this distribution does not substantially change at higher frequencies due to the proximity effect of the other conductor, which opposes the edge effect.

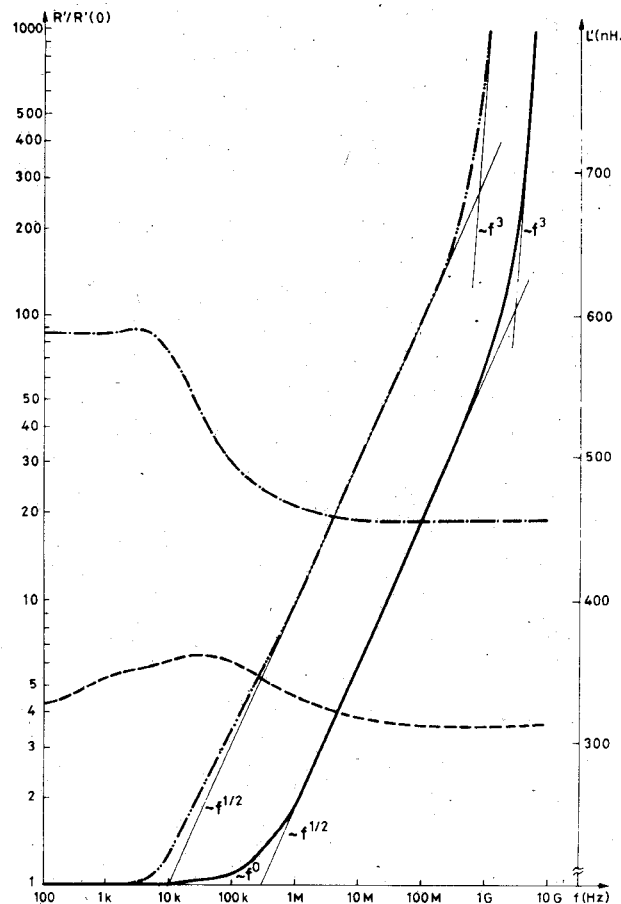


Fig. 6. Normalized resistance per unit length and inductance per unit length of the two analyzed transmission lines of the form shown in Fig. 5 versus frequency. The resistances are normalized with respect to the numerically obtained low-frequency value ($R'(0)$). —, —— resistance and inductance for $a = 1$ mm, $b = 0.1$ mm, and $c = 0.5$ mm; $R'(0) = 86$ m Ω /m; $NX = 8$, $NY = 2$. ·····, ····· resistance and inductance for $a = b = 1$ mm and $c = 2$ mm; $R'(0) = 8.8$ m Ω /m; $NX = NY = 8$.

In order to get an insight into the stability of the present solution, we present in Table I the resistance and inductance per unit length for various numbers of subsections along the longer and shorter sides of the conductor (NX and NY), at three specific frequencies. At 1 kHz, we have a low-frequency case, which is practically identical to the dc case; at 1 MHz, the skin-effect is very pronounced, while, at 1 GHz, the radiation resistance attains a substantial value. It can be seen that at all three frequencies the results do not depend significantly on the number of subsections, and that satisfactory accuracy can be obtained with the same low number of subsections (say, $NX = 8$, $NY = 2$), regardless of the frequency range.

As the second example, the conductors were assumed to be of a square cross section, i.e., $a = b = 1$ mm, while $c = 2$ mm. The resistance and inductance per unit length of this transmission line, versus frequency, are given in Table II and sketched in Fig. 6.

From the above results, it can be seen clearly that the resistance remains constant and equal to the dc resistance (the exact value is 8.93 m Ω /m) up to frequencies when the width of the conductors becomes a significant fraction of

TABLE I
RESISTANCE (R') AND INDUCTANCE (L') PER UNIT LENGTH FOR A
TRANSMISSION LINE OF DIMENSIONS $a = 1$ mm, $b = 0.1$ mm
AND $c = 0.5$ mm, AT THREE FREQUENCIES, FOR VARIOUS
NUMBERS OF PULSES ALONG THE WIDER (NX) AND NARROWER
(NY) SIDE OF THE CONDUCTOR CROSS SECTION

NX	NY	$f = 1$ kHz		$f = 1$ MHz		$f = 1$ GHz	
		R' (m Ω /m)	L' (nH/m)	R' (m Ω /m)	L' (nH/m)	R' (m Ω /m)	L' (nH/m)
2	2	77.98	316.7	163.1	339.0	5874	314.0
4	2	82.12	330.7	158.7	336.5	5640	312.2
8	2	85.86	347.9	163.1	334.2	5730	311.2
8	4	85.34	345.7	162.2	333.9	5822	310.4
16	2	87.74	357.8	174.5	333.6	5732	310.4
16	4	87.60	357.1	175.3	333.9	5790	310.0

TABLE II
RESISTANCE (R') AND INDUCTANCE (L') PER UNIT LENGTH FOR A
TRANSMISSION LINE OF DIMENSIONS $a = b = 1$ mm AND
 $c = 2$ mm VERSUS FREQUENCY.

f (Hz)	R' (m Ω /m)	L' (nH/m)	δ (mm)
100	8.78	586	67
1000	8.78	588	21
10 000	11.02	572	6.7
100 000	30.80	496	2.1
1 000 000	86.00	466	0.67
10 000 000	273.2	456	0.21
100 000 000	874.6	454	0.067
1 000 000 000	7426	454	0.021

The numbers of pulses are $NX = NY = 8$. Skin-depth (δ) is shown for comparison.

the skin-depth. Above these frequencies, we can note the usual square-root behavior of the resistance. The inductance has a frequency region where it decreases, because then the magnetic field in the interior of the conductors is depleted, and the internal inductance becomes very small. In addition, for both conductors, the centroid of the current moves from the center of the cross section towards the other conductor, which also reduces the inductance at higher frequencies.

V. CONCLUSION

A procedure is presented for the numerical analysis of a two-dimensional electromagnetic system, consisting of a number of conductors, made of homogeneous materials, and embedded in a homogeneous dielectric. The excitation of the system was assumed to be uniform along the axis of the system and of the TM nature. The problem was solved by introducing equivalent surface electric and magnetic currents at the interfaces between the conductors and the dielectrics, thus obtaining a number of systems filled with a homogeneous medium. The unknown distributions of the electric and magnetic currents were then determined from coupled integral equations, based on the boundary conditions for the tangential electric and magnetic fields. These equations were solved by the point-matching technique, with pulse approximations of the unknown current distributions. The numerical results obtained for the case of two identical conductors of rectangular cross sections exhibit a relatively good stability and behave according to the predictions, which take into account the proximity, edge, skin

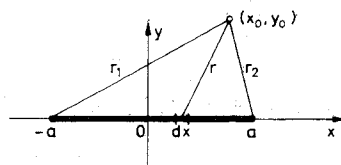


Fig. 7. Coordinate system for evaluation of quasi-static potential and field integrals at a point (x_0, y_0) .

and radiation effects. The present method can easily be extended to the TE excitation, as well as to the analysis of any two-dimensional electromagnetic system filled with arbitrary piecewise homogeneous media.

APPENDIX EVALUATION OF THE MAIN PART OF THE FIELD INTEGRALS

For simplicity, let us consider a strip the cross section of which is along the x -axis, as sketched in Fig. 7. In order to compute the electric and magnetic fields from (3)–(7), one has to evaluate the integrals the kernel of which is either Green's function, or its gradient. Green's functions have a logarithmic singularity, as already stated, so that the main part of the singular integrals to be evaluated is either $-L/4\pi$, where

$$L = \int_{-a}^a \log((x - x_0)^2 + y_0^2) dx$$

$$= \left[(x - x_0) \log((x - x_0)^2 + y_0^2) \right. \\ \left. + 2y_0 \operatorname{arctg} \left(\frac{x - x_0}{y_0} \right) - 2(x - x_0) \right]_{x=-a}^a \quad (18)$$

when evaluating the integral of Green's function, or $-1/4\pi(\partial L/\partial x_0 i_x + \partial L/\partial y_0 i_y)$ when evaluating the integral of $\operatorname{grad} g(r)$. i_x and i_y are unit vectors in the \hat{x} and \hat{y} direction, respectively. In the latter case, we have

$$\frac{\partial L}{\partial x_0} = - \left[\log((x - x_0)^2 + y_0^2) \right]_{x=-a}^a, \quad (19)$$

$$\frac{\partial L}{\partial y_0} = \left[2 \operatorname{arctg} \left(\frac{x - x_0}{y_0} \right) \right]_{x=-a}^a. \quad (20)$$

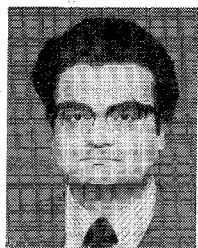
REFERENCES

- [1] J. Venkataraman, S. M. Rao, A. R. Djordjević, T. K. Sarkar, and Y. Naiheng, "Analysis of arbitrarily oriented microstrip transmission lines in arbitrarily shaped dielectric media," this issue.
- [2] C. Wei, R. F. Harrington, J. R. Mautz, and T. K. Sarkar, "Multiconductor transmission lines in multilayered dielectric media," *IEEE Trans. Microwave Theory Tech.*, Vol. MTT-32, pp. 439–450, Apr. 1984.
- [3] R. F. Harrington, *Time-Harmonic Electromagnetic Fields*. New York: McGraw-Hill, 1961.
- [4] B. D. Popović, "Electromagnetic field theorems (a review)," *Proc. Inst. Elec. Eng., A*, pp. 47–63, 1981.
- [5] R. F. Harrington, *Field Computation by Moment Methods*. New York: Macmillan, 1968.



Antonije R. Djordjević was born in Belgrade, Yugoslavia, in 1952. He received the B.Sc., M.Sc., and D.Sc. degrees from the University of Belgrade in 1975, 1977, and 1979, respectively.

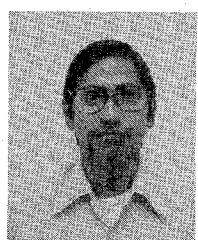
In 1975, he joined the Department of Electrical Engineering, University of Belgrade, as a Teaching Assistant in Electromagnetics. In 1982, he was appointed as Assistant Professor in Microwaves at the same department. From February 1983 until February 1984, he was with the Department of Electrical Engineering, Rochester Institute of Technology, Rochester, NY, as a Visiting Associate Professor. His research interests are numerical problems in electromagnetics, especially those applied to antennas and microwave passive components.



Tapan K. Sarkar (S'69–M'76–SM'81) was born in Calcutta, India, on August 2, 1948. He received the B. Tech. degree from the Indian Institute of Technology, Kharagpur, India, in 1969, the M.Sc.E. degree from the University of New Brunswick, Fredericton, NB, Canada, in 1971, and the M.S. and Ph.D. degrees from the Syracuse University, Syracuse, NY, in 1975.

From 1969 to 1971, he served as an Instructor at the University of New Brunswick. While studying at Syracuse University, he served as an Instructor and Research Assistant in the Department of Electrical Engineering. From 1976 to 1985, he was with Rochester Institute of Technology, Rochester, NY. From 1977 to 1978, he was a Research Fellow at the Gordon McKay Laboratory of Harvard University, Cambridge, MA. Presently, he is with the Department of Electrical and Computer Engineering of Syracuse University, Syracuse, NY. His current research interests deal with numerical solution of operator equations arising in electromagnetics and signal processing with application to system identification.

Dr. Sarkar is a Registered Professional Engineer in the state of New York. He is a member of Sigma Xi and International Union of Radio Science Commissions A and B.



Sadasiva M. Rao (M'83) received the Bachelor's degree in electrical and communication engineering from Osmania University, Hyderabad, India, in 1974, the Masters degree in 1976 from the Indian Institute of Sciences, Bangalore, India, and the Ph.D. degree from the University of Mississippi, University, MS, in 1980.

Since 1976, he has been a Research Assistant in the Department of Electrical Engineering at the University of Mississippi. Currently, he is an Assistant Professor at Rochester Institute of Technology, Rochester, NY. His research interests are in the areas of electromagnetic theory and numerical methods applied to antennas and scattering.